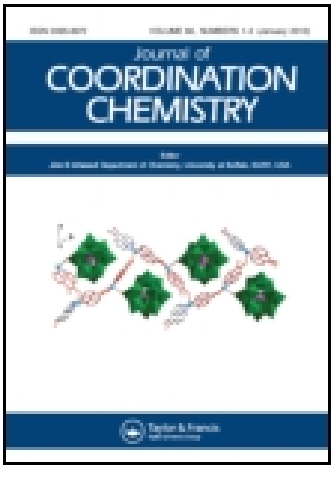

Journal of Coordination Chemistry
Publication details, including instructions for authors and subscription information:
http://www.tandfonline.com/loi/gcoo20

Manganese(II) and silver(I) complexes based on the V-shaped ligand, bis(2-benzimidazolylmethyl)amine: synthesis, crystal structures, DNA-binding properties, and antioxidant activities

Huilu Wu[a], Yanhui Zhang[a], Hua Wang[a], Yuchen Bai[a], Furong Shi[a], Xiaoli Wang[a] & Zaihui Yang[a]

[a] School of Chemical and Biological Engineering, Lanzhou Jiaotong University, Lanzhou, PR China

Accepted author version posted online: 23 Apr 2014.Published online: 20 May 2014.

To cite this article: Huilu Wu, Yanhui Zhang, Hua Wang, Yuchen Bai, Furong Shi, Xiaoli Wang & Zaihui Yang (2014) Manganese(II) and silver(I) complexes based on the V-shaped ligand, bis(2-benzimidazolylmethyl)amine: synthesis, crystal structures, DNA-binding properties, and antioxidant activities, Journal of Coordination Chemistry, 67:10, 1771-1781, DOI: 10.1080/00958972.2014.917632

To link to this article: http://dx.doi.org/10.1080/00958972.2014.917632

Journal of Coordination Chemistry, 2014
Vol. 67, No. 10, 1771–1781, http://dx.doi.org/10.1080/00958972.2014.917632

Manganese(II) and silver(I) complexes based on the V-shaped ligand, bis(2-benzimidazolylmethyl)amine: synthesis, crystal structures, DNA-binding properties, and antioxidant activities

HUILU WU*, YANHUI ZHANG, HUA WANG, YUCHEN BAI, FURONG SHI, XIAOLI WANG and ZAIHUI YANG

School of Chemical and Biological Engineering, Lanzhou Jiaotong University, Lanzhou, PR China

(*Received 13 January 2014; accepted 25 March 2014*)

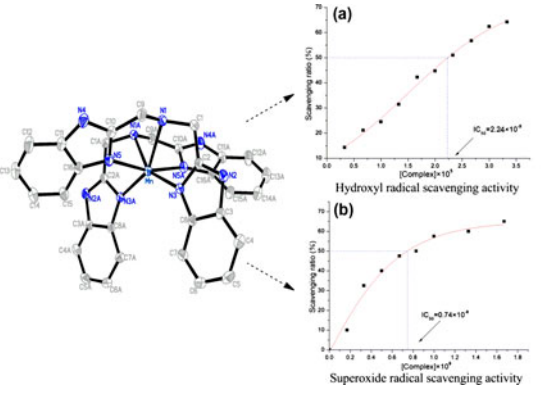

Two Mn(II) and Ag(I) complexes, $[Mn(IDB)_2](pic)_2$ (pic = picrate) (**1**) and $[Ag_2(IDB)_2](pic)_2$ (**2**) (IDB = bis(2-benzimidazolylmethyl)amine), have been synthesized and characterized by elemental analysis, IR, UV–vis spectral measurements, and X-ray single-crystal diffraction. Single-crystal X-ray diffraction revealed that Mn(II) is six-coordinate by six nitrogens from two IDB as a distorted octahedron, and the Ag(I) complex revealed two Ag(I) ions bonded to two IDB ligands through six nitrogens, resulting in an asymmetric binuclear structure. The complexes can bind to DNA through an intercalative mode, and the affinity for DNA is stronger for the Mn(II) complex than the Ag(I) complex; the Mn(II) complex exhibits excellent antioxidative activity.

Keywords: Bis(2-benzimidazolylmethyl)amine; Crystal structure; Manganese(II) complex; Silver(I) complex; DNA-binding property; Antioxidant property

1. Introduction

Compounds containing N-coordinated ligands such as imidazole, benzimidazole, pyridine, or pyrazole as well as thioether or mercapto groups produce different kinds of transition

*Corresponding author. Email: wuhl@mail.lzjtu.cn

metal complexes which exhibit biological (antibacterial, antifungal, and pesticidal) activities [1–3]. Benzimidazole as a ligand toward transition metal ions has been of interest for design of DNA cleaving reagents in a number of biological models [4–8]. Transition metal complexes have attracted attention as catalytic systems for use in oxidation of organic compounds [9], probes in electron transfer reactions involving metalloproteins [10], and intercalators with DNA [11]. Manganese forms complexes and some manganese complexes exhibit excellent biological activities [12]. Considerable attention has been focused on the use of benzimidazole complexes as intercalating agents of DNA [13, 14]. Therefore, transition metal complexes containing a benzimidazole-based ligand are a subject of intensive research for their rich coordination chemistry and established and potential applications [15, 16].

In previous studies [17–20], we investigated the coordinating ability of various benzimidazole ligands and the corresponding transition metal complexes. In this article, a bis(2-benzimidazolylmethyl)amine (IDB) ligand and its Mn(II) and Ag(I) complexes have been synthesized and characterized. The DNA-binding behaviors were investigated by spectrophotometric methods and viscosity measurements. Antioxidant activities of the Mn(II) complex were determined by superoxide ($O_2^{-\cdot}$) and hydroxyl radical ($OH^{\cdot}$) scavenging methods *in vitro*.

2. Experimental setup

2.1. *Physical measurements and materials*

C, H, and N analyses were determined using a Carlo Erba 1106 elemental analyzer. IR spectra were recorded from 4000 to 400 cm^{-1} with a Nicolet FT-VERTEX 70 spectrometer using KBr pellets. Electronic spectra were taken on a Lab-Tech UV Bluestar spectrophotometer. Fluorescence spectra were recorded on a LS-45 spectrofluorophotometer at room temperature. Viscosity experiments were conducted on an Ubbelodhe viscometer, immersed in a thermostated water bath maintained at 25 ± 0.1 °C. The antioxidant activities were performed in a water bath with a 722sp spectrophotometer.

Ethidium bromide (EB) and calf thymus DNA (CT-DNA) were purchased from Sigma-Aldrich and used without purification. EDTA and safranin were purchased in China. $Mn(pic)_2$ and $Ag(pic)_2$ were synthesized from manganese carbonate and silver carbonate with picric acid. Other reagents and solvents were of reagent grade obtained from commercial sources and used without purification. Tris–HCl buffer, Na_2HPO_4–NaH_2PO_4 buffer, and EDTA–Fe(II) solutions were prepared using double distilled water. All the experiments involving interaction of the ligand and the complex with CT-DNA were carried out in double distilled water buffer containing 5 mM Tris and 50 mM NaCl, and adjusted to pH 7.2 with hydrochloric acid. The CT-DNA concentration per nucleotide was determined spectrophotometrically by employing an extinction coefficient of 6600 M^{-1} cm^{-1} at 260 nm [21].

2.2. *DNA-binding study*

The mode of binding of the complexes to CT-DNA was studied with electronic absorption spectroscopy, fluorescence spectroscopy, and viscosity measurements. Absorption titration experiments were performed with fixed concentrations of the complexes, while gradually

increasing the concentration of CT-DNA. To obtain the absorption spectra, the required amount of CT-DNA was added to the solution of the complex and the reference solution to eliminate the absorbance of CT-DNA itself. The binding constant (K_b) was determined using the equation [22]:

$$[\mathrm{DNA}]/(\varepsilon_a - \varepsilon_f) = [\mathrm{DNA}]/(\varepsilon_b - \varepsilon_f) + 1/K_b(\varepsilon_b - \varepsilon_f)$$

The EB competitive experiment was carried out by titrating the complex step by step into EB-DNA complex solution. The influence of the addition of each compound to the EB-DNA complex solution was obtained by recording the variation of the fluorescence emission spectra. Fluorescence spectra of EB were measured using an excitation wavelength of 520 nm, and the emission range was set between 550 and 750 nm. The spectra were analyzed according to the classical Stern–Volmer equation [23]:

$$I_0/I = 1 + K_{sv}[\mathrm{Q}]$$

Viscosity experiments were conducted on an Ubbelohde viscometer, immersed in a water bath maintained at 25.0 ± 0.1 °C. Data are presented as $(\eta/\eta_0)^{1/3}$ *versus* the ratio of the concentration of the compound to CT-DNA, where η is the viscosity of CT-DNA in the presence of the compound and η_0 is the viscosity of CT-DNA alone. Viscosity values were calculated from the observed flow time of CT-DNA-containing solutions corrected from the flow time of the buffer alone (t_0), $\eta = (t - t_0)$ [24].

2.3. *Antioxidant property*

The antioxidant radical scavenging activity of the Mn(II) complex was determined by the superoxide and hydroxyl radical methods *in vitro*. The experimental content is consistent with the reference literature [20].

2.4. *Preparation of the ligand and its complex*

2.4.1. Preparation of bis(2-benzimidazolylmethyl)amine (IDB). IDB was synthesized according to the published procedure [25]. The infrared and UV spectra of IDB were consistent with the literature data [26, 27]. Yield: 2.19 g (59.1%). Calcd (%) for $C_{16}H_{15}N_5$: C, 69.30; H, 5.45; N, 25.26. Found (%): C, 69.35; H, 5.47; N, 25.16. UV–vis (λ, nm): 277, 283. FT-IR (KBr ν/cm^{-1}): 1270 ν(C–N); 1436 ν(C=N); 1620 ν(C=C). ^{1}H NMR (DMSO 300 MHz) δ/ppm: 12.3 (1H, N–H); 7.144 (m, 4H,); 7.5 (d, 4H); 4.0 (s, 4H).

2.4.2. Preparation of Mn(II) complex. To a stirred solution of IDB (0.111 g, 0.40 mM) in hot EtOH (10 mL) was added to a solution of $Mn(pic)_2$ (0.102 g, 0.2 mM) in MtOH (2 mL). A yellow crystalline product formed rapidly. The precipitate was filtered off, washed with EtOH and absolute Et_2O, and dried in *vacuo*. The dried precipitate was dissolved in EtOH to form a yellow solution into which Et_2O was allowed to diffuse at room temperature. Crystals suitable for X-ray measurements were obtained after four weeks. Yield: 0.123 g (57.7%). Calcd (%) for $C_{44}H_{34}MnN_{16}O_{14}$: C, 49.54; H, 3.19; N, 21.02. Found (%): C, 49.62; H, 3.10; N, 21.31. UV–vis (λ, nm): 275, 286, 379. FT-IR (KBr ν/cm^{-1}): 1274 ν(C–N); 1451 ν(C=N); 1635 ν(C=C).

2.4.3. Preparation of Ag(I) complex. IDB (0.111 g, 0.4 mM) and silver (I) picrate (0.134 g, 0.4 mM) were dissolved in methanol (10 mL). The reaction mixture was stirred for 4 h. The precipitate was filtered off, washed with MeOH and absolute Et_2O, and dried in *vacuo*. The product was dissolved in MeCN to form a yellow solution that was allowed to evaporate at room temperature. Yellow crystals suitable for X-ray diffraction were obtained after two weeks. Yield: 0.132 g (53.8%). Calcd (%) for $C_{44}H_{32}Ag_2N_{16}O_{14}$: C, 43.11; H, 2.61; N, 18.29. Found (%): C, 43.17; H, 2.58; N, 18.52. UV–vis (λ, nm): 275, 280, 407. FT-IR (KBr ν/cm^{-1}): 1276 ν(C–N); 1456 ν(C=N); 1622 ν(C=C).

2.5. *X-ray crystallography*

A suitable single-crystal was mounted on a glass fiber and the intensity data were collected on a Bruker Smart CCD diffractometer with graphite-monochromated Mo Kα radiation ($\lambda = 0.71073$ Å) at 296(2) K. Data reduction and cell refinement were performed using the SMART and SAINT programs [28]. The structure was solved by Direct Methods and refined by full-matrix least squares against F^2 of data using SHELXTL software [29]. All hydrogens were found in difference electron maps and were subsequently refined in a riding-model approximation with C–H distances ranging from 0.93 to 0.97 Å and $U_{iso}(H) = 1.2\ U_{eq}(C)$. Basic crystal data, details of the diffraction experiment, and the structure refinement are given in table 1. Selected atomic distances and angles of the complexes are listed in table 2.

Table 1. Crystal and structure refinement data for **1** and **2**.

Complex	**1**	**2**
Molecular formula	$C_{44}H_{34}MnN_{16}O_{14}$	$C_{44}H_{34}Ag_2N_{16}O_{14}$
Molecular weight	1065.81	1226.61
Crystal system	Monoclinic	Monoclinic
Space group	*C2/c*	*P2(1)/n*
a (Å)	23.852(7)	10.2046(10)
b (Å)	9.691(3)	18.2502(17)
c (Å)	21.422(7)	25.056(2)
β (°)	118.591(2)	96.6220(10)
V (Å^3)	4348(2)	4635.3(8)
Z	4	4
D (Calcd)(g cm^{-3})	1.628	1.76
F (0 0 0)	2188	2464
Crystal size (mm)	0.36 × 0.34 × 0.32	0.4 × 0.38 × 0.3
θ Range for data collection	2.17–25.5	1.98–25.50
h/*k*/*l* (max, min)	−28,28/−11,11/−25,25	−12,12/−22,20/−25,30
Reflections collected	15,260	24,463
Independent reflections	4053/0.0529	8617/0.0213
Refinement method	Full-matrix least-squares on F^2	Full-matrix least-squares on F^2
Data/restraints/parameters	4053/0/343	8617/0/685
Goodness-of-fit on F^2	1.007	0.0291/0.0698
Final R_1, wR_2 indices [$I > 2\sigma(I)$]	0.0469/0.0992	0.0370/0.0737
R_1, wR_2 indices (all data)	0.0812/0.1137	1.039
Largest diff. peak and hole (e Å^{-3})	0.593/−0.373	0.57/−0.51

Table 2. Selected bond lengths (Å) and angles (°) of **1** and **2**.

1			
Mn–N(5)	2.218(2)	Mn–N(1)#1	2.385(3)
Mn–N(5)#1	2.218(2)	Mn–N(3)#1	2.227(2)
Mn–N(3)	2.227(2)	Mn–N(1)	2.385(3)
N(5)–Mn–N(5)#1	165.20(13)	N(3)–Mn–N(1)#1	152.74(8)
N(5)–Mn–N(3)	97.13(9)	N(3)#1–Mn–N(1)#1	72.50(9)
N(5)#1–Mn–N(3)	88.85(9)	N(5)–Mn–N(1)	74.93(9)
N(5)–Mn–N(3)#1	88.85(9)	N(5)#1–Mn–N(1)	94.17(9)
N(5)#1–Mn–N(3)#1	97.13(9)	N(3)–Mn–N(1)	72.50(9)
N(3)–Mn–N(3)#1	132.27(12)	N(3)#1–Mn–N(1)	152.74(8)
N(5)–Mn–N(1)#1	94.17(9)	N(5)#1–Mn–N(1)#1	74.93(9)
N(1)#1–Mn–N(1)	86.74(13)		
2			
Ag(1)–N(5)	2.162(2)	Ag(2)–N(6)	2.717(2)
Ag(1)–N(8)	2.122(2)	Ag(1)–Ag(2)	3.0809(4)
Ag(2)–N(10)	2.140(2)	Ag(2)–N(3)	2.1356(19)
Ag(1)–N(1)	2.563(2)		
N(5)–Ag(1)–N(8)	155.02(8)	N(10)–Ag(2)–N(3)	157.52(9)
N(8)–Ag(1)–N(1)	130.55(7)	N(3)–Ag(2)–N(6)	130.45(7)
N(5)–Ag(1)–N(1)	73.03(7)	N(10)–Ag(2)–N(6)	70.19(8)
N(8)–Ag(1)–Ag(2)	78.34(6)	N(10)–Ag(2)–Ag(1)	101.56(7)
N(5)–Ag(1)–Ag(2)	93.99(6)	N(3)–Ag(2)–Ag(1)	74.10(6)
N(1)–Ag(1)–Ag(2)	93.02(5)	N(6)–Ag(2)–Ag(1)	87.09(5)

Note: Symmetry transformations used to generate equivalent atoms: #1 $-x, y, -z + 1/2$.

3. Results and discussion

The two complexes are soluble in polar aprotic solvents such as DMF and DMSO, slightly soluble in ethanol, methanol, ethyl acetate, and chloroform, and insoluble in water, Et_2O, and petroleum ether. The elemental analyses show that the compositions are $[Ag_2(IDB)_2](pic)_2$ and $[Mn(IDB)_2](pic)_2$, which were confirmed by crystal structure analysis.

3.1. *IR and electronic spectra*

IR spectra of the free ligand and the two complexes were recorded and assigned. IDB shows absorptions of benzimidazole at 1270, 1436, and 1620 cm^{-1} assigned to ν(N–C), ν(C=N), and ν(C=C), respectively [30]. Two bands were found at 1274 and 1451 cm^{-1} for the Mn(II) complex, shifted 4–15 cm^{-1}, the location of the band is slightly shifted for the Ag(I) complex, with 1436 cm^{-1} shifted to 1456 cm^{-1}, attributed to coordination of benzimidazole nitrogen [31]. Information regarding the possible bonding modes of picrate and benzimidazole rings may be obtained from IR spectra, such as 709, 742, 744, 1272, 1334, 1336, and 1633 cm^{-1}. This agrees with the result determined by X-ray diffraction.

DMF solutions of IDB and of the complexes show, as expected, almost identical UV spectra. The UV bands of IDB (277, 283 nm) are only marginally shifted by 2–3 nm in the two complexes, clear evidence of C=N coordination. These bands are assigned to $\pi \rightarrow \pi^*$ (imidazole) transitions [32]. A new absorption at (379, 407 nm) in the Mn(II) and Ag(I) complexes is attributed to $\pi \rightarrow \pi^*$ (Pic) transitions.

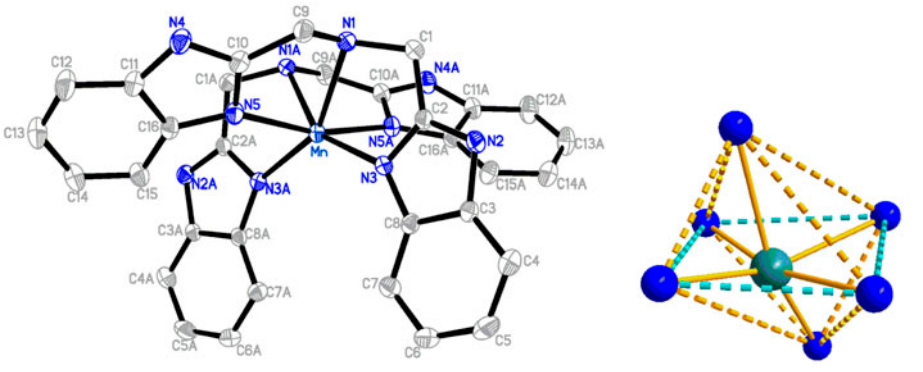

Figure 1. The Mn(II) showing displacement ellipsoids at the 30% probability level. Hydrogens and anion omitted for clarity.

3.2. *X-ray structures of [Mn(IDB)$_2$](pic)$_2$ and [Ag$_2$(IDB)$_2$](pic)$_2$*

On the basis of single-crystal X-ray analysis of [Mn(IDB)$_2$](pic)$_2$, Mn is located at the center of a distorted octahedron, which consists of six nitrogens from two ligands. The Mn(II) complex crystallized in the monoclinic lattice with a *C2/c* space group.

The molecular structure of the Mn(II) complex is shown in figure 1. The coordination geometry of Mn(II) may be best described as distorted octahedral with four benzimidazole nitrogens (N3, N5, N1A, and N5A) from an equatorial plane. The axial positions are occupied by IDB N1 and another IDB N3A. The distance between the axial N3A and the equatorial plane is 2.188 Å, but the distance between the axial N1 and the equatorial plane is 2.385 Å. The shortest Mn–N bond length is 2.218(2) Å and the longest is 2.385(3) Å. The bond angle of N1 and N3A in axial positions is 152.74(8)°. Compared with a regular octahedron, the bond lengths and bond angles show distortion. In the crystal, adjacent picrate rings are concatenated by $\pi\cdots\pi$ interactions ($d = 3.673$ Å), adjacent benzimidazole rings and picrates are concatenated by $\pi\cdots\pi$ interactions ($d = 3.783$ Å). As shown in figure 2, an S-shaped, 1-D chain is formed by $\pi\cdots\pi$ interactions which increase the stability of the crystal packing.

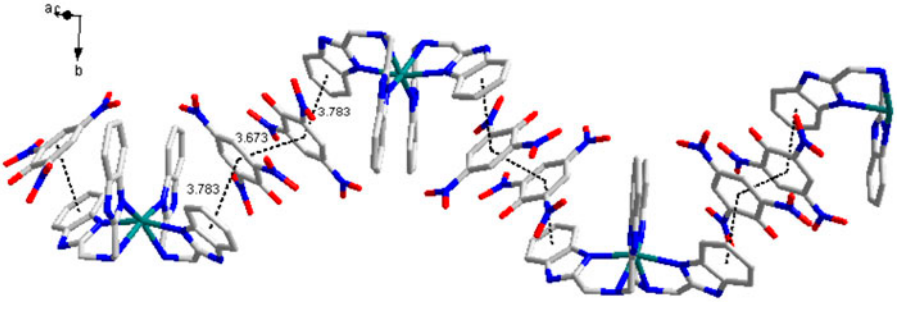

Figure 2. π–π stacking interactions and S-shaped, 1-D chain in Mn(II) complex (for clarity, selected atoms were omitted).

The molecular structure of the silver(I) complex is shown in figure 3. In the complex, two Ag(I) ions and IDB ligands form a binuclear $[Ag_2(IDB)_2](pic)_2$, and two IDB ligands take the shape of a semi-cross. There exists a Ag(1)···Ag(2) bond in the asymmetric unit (Ag(1)···Ag(2) = 3.0809(4) Å), which is similar to our previous reports [33]. Each silver(I) is coordinated by two nitrogens (Ag(1)–N(1) = 2.563(2) and Ag(1)–N(5) = 2.162(2) Å, Ag(2)–N(10) = 2.140(2) and Ag(2)–N(6) = 2.717(2) Å) from one ligand, as well as one nitrogen (Ag(1)–N(8) = 2.122(2) and Ag(2)–N(3) = 2.1356(19) Å) from the other ligand. Thus, each silver(I) ion is AgN_3 trigonal planar, with a Ag···Ag contact roughly perpendicular to this plane. In the crystal, adjacent benzimidazole rings and picrates are concatenated by $\pi\cdots\pi$ interactions (d = 3.592(0) Å), extending along the a axis, as shown in figure 4. In addition, hydrogen bonds (N–H···O) are formed along the b axis, which also contribute to the stability of the structure.

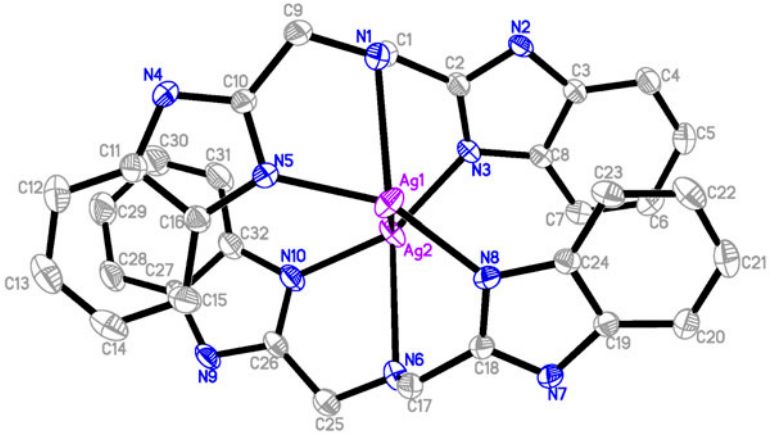

Figure 3. The cation of the Ag(I) complex showing displacement ellipsoids at the 30% probability level. Hydrogens and anions are omitted for clarity.

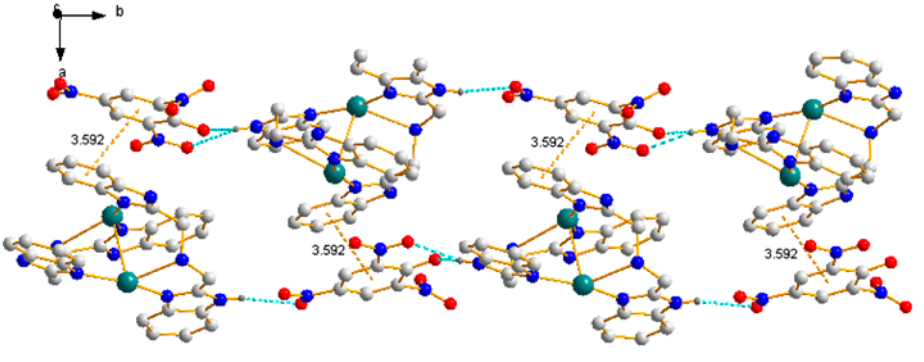

Figure 4. π–π stacking interactions and weak O···H–N hydrogen bonding in the crystal of the complex (for clarity, selected atoms were omitted).

3.3. *DNA-binding properties*

3.3.1. Electronic absorption. Electronic absorption spectroscopy is a powerful experimental technique for probing metal ion–DNA interactions. Absorption titration can monitor the interaction of a compound with DNA. The obvious hypochromism and red shift are usually characterized by non-covalent intercalation of a compound to the DNA helix, due to the strong stacking interaction between the aromatic chromophore of the compound and the base pairs of DNA [34].

Electronic absorption spectra of the two complexes in the absence and presence of CT-DNA are given in figure S1 (see online supplemental material at http://dx.doi.org/10.1080/00958972.2014.917632). With increasing DNA concentration, the absorption at 273 nm of the Mn(II) complex exhibits hypochromism of 23.26%. K_b is given by the ratio of the slope to the intercept. K_b value of the Mn(II) complex is $(4.33 \pm 0.035) \times 10^4\,M^{-1}$ ($R = 0.98$ for 10 points), which is consistent with the hypochromism degree. The absorption band of the Ag(I) complex at 280 nm exhibits hypochromism of 25.9%. It is a general observation that hypochromicity in the absorption spectra accompanies the binding of molecules to DNA. The extent of the spectral change is related to the strength of binding [35]. From the results of the electronic absorption spectroscopy, the binding constant K_b for the Ag(I) complex from the plot of [DNA]/($\varepsilon_a - \varepsilon_f$) *versus* [DNA] is $(2.3 \pm 0.045) \times 10^4\,M^{-1}$ ($R = 0.96$ for nine points). The results indicate that the binding strength of the two complexes follows the order: Mn(II) > Ag(I). Compared with those of the so-called DNA-intercalative ruthenium complexes ($1.1 \times 10^4 - 4.8 \times 10^4\,M^{-1}$) [36], we can conclude that the Mn(II) and Ag(I) complexes interact with CT-DNA in the intercalation mode, which may be due to the large coplanar aromatic rings in the complex that facilitate its intercalation with the base pairs of the double helical DNA. The order of DNA-binding affinity may be explained by the Mn(II) complex being an S-shaped, 1-D polymer chain formed by $\pi\cdots\pi$ interactions, which is conducive to the DNA binding.

3.3.2. Fluorescence spectroscopy. EB emits intense fluorescence in the presence of CT-DNA, due to its strong intercalation between the adjacent CT-DNA base pairs. It is reported that the loss of fluorescence intensity at the maximum wavelength indicates displacement of EB from EB-DNA complex by a compound and the intercalative binding between the compounds with DNA [37]. The changes observed in the spectra of EB on its binding to CT-DNA are often used for the interaction study between DNA and other compounds, such as metal complexes [38]. The effect of a complex with the EB-DNA complex was studied by adding a certain amount of a solution of the complex step by step into the buffer solution of the EB-DNA complex [39].

The emission spectra of the EB-DNA system in the absence and presence of the Mn(II)/Ag(I) complexes are displayed in figure S2. The behavior of the Mn(II)/Ag(I) complexes is in agreement with the Stern–Volmer equation, which provides further evidence that there are interactions between the complexes and DNA. The K_{sv} values for **1** and **2** were $(7.6 \pm 0.050) \times 10^4\,M^{-1}$ ($R = 0.97$ for seven points) and $(3.91 \pm 0.036) \times 10^4\,M^{-1}$ ($R = 0.98$ for eight points). The values of the complexes show that they can displace EB and bind to DNA [40–43]. The data show that the interaction of the Mn(II) complex with DNA is stronger than that of the Ag(I) complex, which is consistent with the above absorption.

3.3.3. Viscosity measurements. To further explore the interaction between the metal complexes and DNA, the relative specific viscosity of DNA was examined by varying the concentration of the added metal complexes. Hydrodynamic measurements that are sensitive to length change (i.e. viscosity and sedimentation) are regarded as the least ambiguous and the most critical tests of binding in solution in the absence of crystallographic structural data [44]. The effects of the two complexes on the viscosity of DNA at 25.0 °C are shown in figure S3. The viscosity of the DNA increases steadily with increasing amounts of **1** or **2**. As shown in figure S3, the Mn(II) complex can intercalate more deeply than the Ag(I) complex. The results obtained from viscosity studies also validate those obtained from the spectroscopic studies. Therefore, we draw the conclusion that complexes can bind to DNA in an intercalative mode.

3.4. *Antioxidant activities*

3.4.1. Hydroxyl radical scavenging activity. Mannitol is a well-known natural antioxidant, so we also studied the scavenging activity of mannitol against hydroxyl radicals using the same mode [45]. The 50% inhibitory concentration (IC_{50}) value of mannitol is about 9.6×10^{-3} M. According to the antioxidant experiments, the IC_{50} of the Mn(II) complex is 2.24×10^{-5} M [figure 5(a)], which implies that the Mn(II) complex exhibits better scavenging activity than mannitol. It was believed that the information obtained from the present work would be useful to develop new potential antioxidants and therapeutic agents for some diseases.

3.4.2. Superoxide radical scavenging activity. As another significant assay of antioxidant activity, superoxide ($O_2^{-\cdot}$) scavenging activity of the title complexes has been investigated. Complex **1** has good superoxide radical scavenging activity, but **2** and IDB do not have activity. As can be seen from figure 5(b), the Mn(II) complex shows an IC_{50} value of 0.74×10^{-6} M, which indicates that it has potent scavenging activity for the superoxide radical ($O_2^{-\cdot}$) and may act as an inhibitor (or a drug) to scavenge superoxide radicals *in vivo*, which needs further investigation.

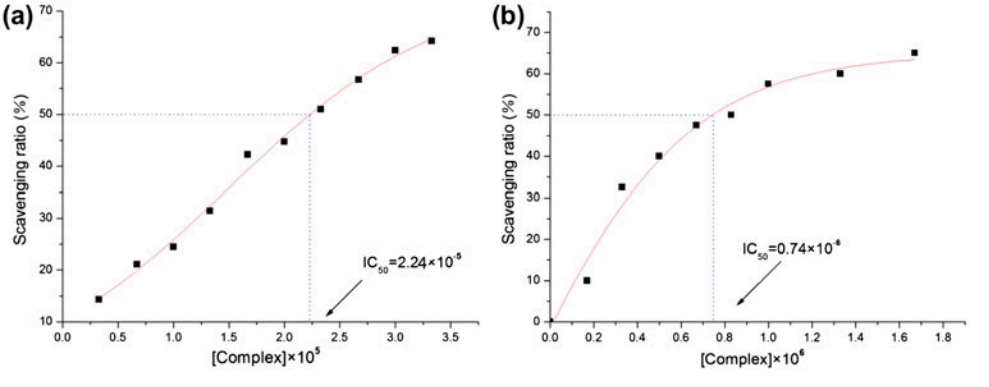

Figure 5. Plots of antioxidation properties for the Mn(II) complex; (a) represents the hydroxyl radical scavenging effect (%) for the Mn(II) complex; (b) represents the superoxide radical scavenging effect (%) for the Mn(II) complex.

4. Conclusion

In this article, new Mn(II) and Ag(I) complexes have been synthesized and characterized. The structures of the two complexes were determined on the basis of elemental analyses, molar conductivities, IR spectra, UV–vis spectra, and X-ray crystallography. The DNA-binding experiments suggest that the two complexes bind to DNA in an intercalation mode, which may be due to charge transfer and reduction of the charge density of the planar conjugated system upon coordination to the metal complex. The binding strength of the two complexes follows the order: Mn(II) > Ag(I). Additionally, the Mn(II) complex exhibited antioxidant activities against $OH^{\cdot}$ and $O_2^{-\cdot}$ radicals *in vitro*. These findings will be helpful to understanding of the mechanism of interactions with DNA and should be useful in the development of new therapeutic reagents for diseases on the molecular level and warrant further *in vivo* experiments and pharmacological assays.

Supplementary material

Crystallographic data (excluding structure factors) for the structure reported in this article have been deposited with the Cambridge Crystallographic Data Center with reference numbers CCDC 950643 and 932318. Copies of the data can be obtained, free of charge, on application to the CCDC, 12 Union Road, Cambridge CB2 1EZ, UK. Tel: +44 01223 762910; Fax: +44 01223 336033; E-mail: deposit@ccdc.cam.ac.uk or http://www.ccdc.cam.ac.uk.

Funding

The present research was supported by the National Natural Science Foundation of China [grant number 21367017]; the Fundamental Research Funds for the Gansu Province Universities [grant number 212086]; National Natural Science Foundation of Gansu Province [grant number 1212RJZA037]; 'Qing Lan' Talent Engineering Funds for Lanzhou Jiaotong University.

References

[1] A. Jouaiti, N. Kyritsakas, J.M. Planeix, M.W. Hosseini. *CrystEngComm*, **8**, 883 (2006).
[2] A.Y. Robin, J.L. Sagué, K.M. Fromm. *CrystEngComm*, **8**, 403 (2006).
[3] F. Arjmand, S. Parveen, M. Afzal, M. Shahid. *J. Photochem. Photobiol., B*, **114**, 15 (2012).
[4] Y. Zhang, R. Yang, F. Liu, K. Li. *Anal. Chem.*, **76**, 7336 (2004).
[5] J. Sisko, A.J. Kassick, M. Mellinger, J.J. Filan, A. Allen, M.A. Olsen. *J. Org. Chem.*, **65**, 1516 (2000).
[6] H.L. Wu, J.K. Yuan, Y. Bai, G.L. Pan, H. Wang, X.B. Shu, G.Q. Yu. *J. Coord. Chem.*, **65**, 616 (2012).
[7] W.K. Pogozelski, T.D. Tullius. *Chem. Rev.*, **98**, 1089 (1998).
[8] C. Tu, Y. Shao, N. Gan, Q. Xu, Z. Guo. *Inorg. Chem.*, **43**, 4761 (2004).
[9] C. Kokubo, T. Katsuki. *Tetrahedron*, **52**, 13895 (1996).
[10] S. Schoumacker, O. Hamelin, J. Pécaut, M. Fontecave. *Inorg. Chem.*, **42**, 8110 (2003).
[11] C.M. Dupureur, J.K. Barton. *Inorg. Chem.*, **36**, 33 (1997).
[12] E.J. Gao, L. Lin, B. Wang, M.C. Zhu, W. Jiao, T.L. Liu. *J. Coord. Chem.*, **66**, 1945 (2013).
[13] J.A. Zhao, S.S. Li, D.D. Zhao, S.F. Chen, J.Y. Hu. *J. Coord. Chem.*, **66**, 1650 (2013).
[14] H.L. Wu, J.K. Yuan, Y. Bai, G.L. Pan, H. Wang, J.H. Shao, J.L. Gao, Y.Y. Wang. *J. Coord. Chem.*, **65**, 4327 (2012).
[15] J.A. Cowan. *Chem. Rev.*, **98**, 1067 (1998).
[16] C.L. Liu, M. Wang, T.L. Zhang, H.Z. Sun. *Coord. Chem. Rev.*, **248**, 147 (2004).
[17] H.L. Wu, K. Li, T. Sun, F. Kou, F. Jia, J.K. Yuan, B. Liu, B.L. Qi. *Transition Met. Chem.*, **36**, 21 (2011).
[18] H.L. Wu, X.C. Huang, B. Liu, F. Kou, F. Jia, J.K. Yuan, Y. Bai. *J. Coord. Chem.*, **64**, 4383 (2011).
[19] H.L. Wu, J.K. Yuan, Y. Bai, H. Wang, G.L. Pan, J. Kong. *J. Photochem. Photobiol., B*, **116**, 13 (2012).

[20] G.L. Pan, Y.C. Bai, H. Wang, J. Kong, F.R. Shi, Y.H. Zhang, X.L. Wang, H.L. Wu. *Z. Naturforsch.*, **68b**, 257 (2013).
[21] Y.Q. Wang, B.P. Tang, H.M. Zhang, Q.H. Zhou, G.C. Zhang. *J. Photochem. Photobiol., B*, **94**, 183 (2009).
[22] C. Behrens, N. Harrit, P.E. Nielsen. *Bioconjugate Chem.*, **12**, 1021 (2001).
[23] M. Shakir, M. Azam, M.F. Ullah, S.M. Hadi. *J. Photochem. Photobiol., B*, **104**, 449 (2011).
[24] C.P. Tan, J. Liu, L.M. Chen, S. Shi, L.N. Ji. *J. Inorg. Biochem.*, **102**, 1644 (2008).
[25] H.P. Berends, D.W. Stephan. *Inorg. Chim. Acta*, **93**, 173 (1984).
[26] J.B. Chaires, N. Dattagupta, D.M. Crothers. *Biochemistry*, **21**, 3933 (1982).
[27] H.L. Wu, K.T. Wang, B. Liu, F. Kou, F. Jia, J.K. Yuan, Y. Bai. *Inorg. Chim. Acta*, **384**, 302 (2012).
[28] Bruker. *SMART, SAINT and SADABS*, Bruker Axs, Inc., Madison, WI (2000).
[29] G.M. Sheldrick. *SHELXTL*, Siemens Analytical X-ray Instruments, Inc., Madison, WI (1996).
[30] C.Y. Su, B.S. Kang, C.X. Du, Q.C. Yang, T.C.W. Mak. *Inorg. Chem.*, **39**, 4843 (2000).
[31] W.K. Dong, Y.X. Sun, L. Li, S.T. Zhang, L. Wang, X.Y. Dong, X.H. Gao. *J. Coord. Chem.*, **65**, 2332 (2012).
[32] H.L. Wu, J.K. Yuan, Y. Bai, F. Kou, F. Jia, B. Liu. *Bioinorg. Chem. Appl.*, **2011**, 705989 (2011).
[33] H.L. Wu, J.K. Yuan, Y. Bai, G.L. Pan, H. Wang, J. Kong, X.Y. Fan, H.M. Liu. *Dalton Trans.*, 8829 (2012).
[34] H.L. Lu, J.J. Liang, Z.Z. Zeng, P.X. Xi, X.H. Liu, F.J. Chen, Z.H. Xu. *Transition Met. Chem.*, **32**, 564 (2007).
[35] Z.D. Xu, H. Liu, S.L. Xiao, M. Yang, X.H. Bu. *J. Inorg. Biochem.*, **90**, 79 (2002).
[36] Y.J. Liu, H. Chao, J.H. Yao, H. Li, Y.Y. Yuan, L.N. Ji. *Helv. Chim. Acta*, **87**, 3119 (2004).
[37] B.D. Wang, Z.Y. Yang, P. Crewdson, D.Q. Wang. *J. Inorg. Biochem.*, **101**, 1492 (2007).
[38] C. Metcalfe, J.A. Thomas. *Chem. Soc. Rev.*, **32**, 215 (2003).
[39] A. Tarushi, G. Psomas, C.P. Raptopoulou, V. Psycharis, D.P. Kessissoglou. *Polyhedron*, **28**, 3272 (2009).
[40] A. Tarushi, G. Psomas, C.P. Raptopoulou, D.P. Kessissoglou. *J. Inorg. Biochem.*, **103**, 898 (2009).
[41] K.C. Skyrianou, E. Efthimiadou, V. Psycharis, A. Terzis, D.P. Kessissoglou, G. Psomas. *J. Inorg. Biochem.*, **103**, 1617 (2009).
[42] K.C. Skyrianou, F. Perdih, I. Turel, D.P. Kessissoglou, G. Psomas. *J. Inorg. Biochem.*, **104**, 740 (2010).
[43] A. Tarushi, C.P. Raptopoulou, V. Psycharis, A. Terzis, G. Psomas, D.P. Kessissoglou. *Bioorg. Med. Chem.*, **18**, 2678 (2010).
[44] M. Chauhan, K. Banerjee, F. Arjmand. *Inorg. Chem.*, **46**, 3072 (2007).
[45] T.R. Li, Z.Y. Yang, B.D. Wang, D.D. Qin. *Eur. J. Med. Chem.*, **43**, 1688 (2008).